Electron heating effects in diffusive metal wires

M. Henny, H. Birk, R. Huber, C. Strunk, A. Bachtold et al.

Related Articles

Additional information on Appl. Phys. Lett.

Electron heating effects in diffusive metal wires

M. Henny,[a] H. Birk, R. Huber, C. Strunk, A. Bachtold, M. Krüger, and C. Schönenberger
Institut für Physik, Universität Basel, CH-4056 Basel, Switzerland

We have investigated the electron heating in metallic diffusive wires of varying length at liquid-helium temperature by measuring the electric noise. The local increase of the electron temperature can be essential already for small currents and is well described by a heat-diffusion equation for the electrons. Depending on the electron thermal conductance and the electron–phonon coupling in the wire, different length regimes are identified. The quantitative knowledge of the electron temperature is important for analysis of nonequilibrium effects involving current heating in mesoscopic wires. © *1997 American Institute of Physics.* [S0003-6951(97)01532-5]

If an electrical current flows through a mesoscopic wire, the electron temperature rises above the phonon temperature. Especially at low temperatures, this increase can be substantial and may influence the measurements of electronic transport properties.

Molenkamp and de Jong[1] measured the local electron temperature in a two-dimensional electron gas quantum wire under dc bias current using the thermopower of a quantum point contact. Mittal *et al.*[2] estimated the electron temperature from the electrical resistance by exploiting the known temperature dependence of the weak localization. Another direct tool for the determination of the electron temperature, which is used in this work, is provided by electric-noise measurements.[3]

The electric current that flows through a conductor displays intrinsic temporal fluctuations known as noise.[4] Provided the $1/f$ noise of the resistance R is negligible, the spectral-power density of the current fluctuations S_I (abbreviated as noise in the following) is frequency independent.[5] In thermodynamical equilibrium at temperature T, when the time-averaged current I is zero: $S_I = 4kT/R$ (Johnson–Nyquist noise).[4] Even for $I \neq 0$, the electrons are still in local equilibrium if the wire length L is much larger than the inelastic electron–electron scattering length l_{e-e}. Hence, the electrons still assume a Fermi–Dirac distribution, albeit with a spatially varying electron temperature T_e, which is increased above the phonon temperature T_{ph}. In this hot-electron regime, the noise is determined by the *mean* electron temperature $S_I = 4k\langle T_e \rangle/R$. In the steady state, the current heating is balanced by the electronic heat conduction to the contact pads [Fig. 1(a)] and by the heat transfer to the phonon system, which is determined by the electron–phonon scattering length l_{e-ph}. For large applied voltages $V \gg kT_{ph}/e$, two limiting cases can be distinguished: $\langle T_e \rangle$ is either proportional to V if $L \ll l_{e-ph}$,[6] or to $V^{2/5}$ if $L \gg l_{e-ph}$.[3,7] In the present work, we bridge the gap between these limiting cases by experiments, which are compared to theoretical predictions.[8]

Using standard e-beam lithography, we fabricated Au wires with a length ranging from 0.84 to 200 μm on oxidized Si wafers. In a first step, a 2 nm Ti layer was evaporated under a tilt angle of 30° to provide good adhesion for the contact pads. In a second step, 20 nm Au films were deposited under perpendicular evaporation [Fig. 1(b)]. In a third step, 200 nm Au films were evaporated again under a tilt angle of 30°. The tilt angle of the first and third step was adjusted to the undercut angle such that no material was deposited in the wire region [Fig. 1(c)]. The large, thick Au pads served on the one hand as thermal reservoirs for the electrons and on the other hand as contacts for ultrasonic wire bonding.

The 20 nm thick Au films had a typical sheet resistance of $R_\square \simeq 1.7$ Ω at 2 K, at which temperature the noise measurements were done. The voltage across the wire was amplified with a gain of 1000 by two independent low-noise preamplifiers (EG&G 5184) operating at room temperature. The noise spectrum was obtained by a cross correlation of the two amplifier signals using a spectrum analyzer (HP 89410A). For every data point, the signal was averaged in a frequency interval of 20 kHz at a typical frequency of 400 kHz, where contributions from $1/f$ noise and other noise sources can be neglected. The absolute amplitude of the noise signal was calibrated for every wire against thermal noise at zero current and temperatures ranging from 2 to 10 K. While the sensitivity of our measurement setup for noise can be better than 2×10^{-21} V^2 s for large signals, there is a cutoff at a value of 2×10^{-20} V^2 s, below which the measurement accuracy drops. This cutoff corresponds to the thermal noise of a 180 Ω resistor at 2 K. Since voltage noise is
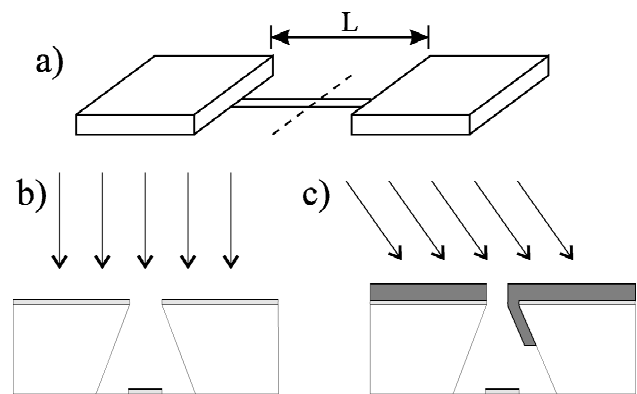

FIG. 1. (a) Schematic of the wire fabricated for noise measurements; (b) perpendicular evaporation of the wire material, (c) evaporation of thick reservoirs under a tilt angle; and (b) and (c) are cross sections along the dashed line in (a).

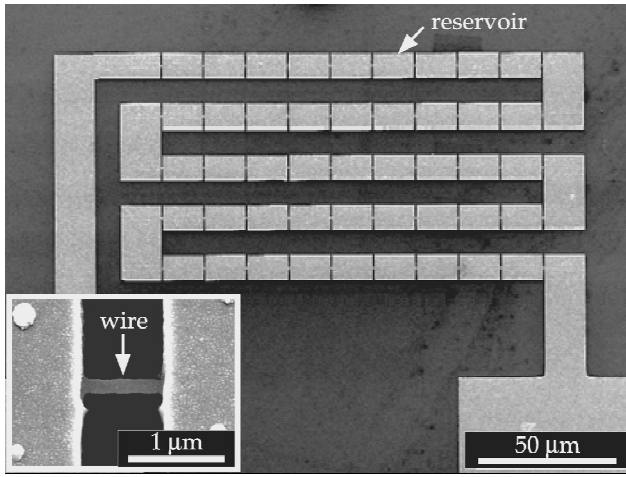[a]Electronic mail: henny@ubaclu.unibas.ch

FIG. 2. 50 wires with a length of 840 nm and a width of 140 nm each with large, thick thermal reservoirs in between, were fabricated using the technique illustrated in Fig. 1. The inset shows one single wire.

FIG. 3. Measured noise power and corresponding electron temperature versus applied electric field for three different samples. Sample A is a 50 μm long Au wire ($R=812\,\Omega$, width $w=110$ nm), sample B consists of five wires of 10 μm length in series ($R=667\,\Omega$, $w=120$ nm), sample C consists of 30 wires with a length of 0.84 μm ($R=300\,\Omega$, $w=140$ nm). a–c correspond to samples A–C, respectively. The typical current range is 45 μA. The thickness of the Au films is 20 nm, and its sheet resistance $R_\square \simeq 1.7\,\Omega$ at the measuring temperature $T=2$ K (A,B) and $T=2.2$ K (C). The solid lines are fits using Eq. (1). The inset shows the calculated temperature profiles along the wire for the three different samples for $\epsilon=160\ \mu$V/μm.

proportional to R, this implies a lower limit for the resistance and for the wire length of about 5 μm for a 50 nm wide Au wire. To overcome this limit, a series of up to 50 equal short wires were fabricated with reservoirs in between (Fig. 2) using the angle evaporation technique described above. The noise signal of a single wire is multiplied by the number of wires allowing the measurement of wires shorter than 1 μm.

Figure 3 shows the spectral density of the noise and the corresponding mean electron temperature versus the applied electric-field ϵ for three different samples (A–C) representing three different length regimes. For better comparison of samples with different resistances, we have plotted $S_I R = 4k\langle T_e\rangle$. The electric field determines the amount of energy locally transferred to the electron gas. Symbols denote measurement points and solid curves are theoretical fits. Sample A is a 50 μm Au wire ($L\gg l_{e-ph}$), sample B consists of five wires of 10 μm length ($L\simeq l_{e-ph}$), and sample C consists of 30 wires of 0.84 μm length ($L\ll l_{e-ph}$).

The noise behavior of all these regimes can be quantitatively explained by a nonlinear differential equation, which describes the spatial dependence of the electron temperature in a wire,[8]

$$\frac{\pi^2}{6}\frac{d^2 T_e^2}{dx^2} = -\left(\frac{e\epsilon}{k_B}\right)^2 + \Gamma(T_e^5 - T_{ph}^5),\qquad(1)$$

where the parameter Γ is related to the electron–phonon scattering length $l_{e-ph}=1.31/\sqrt{T_e^3\Gamma}$ (Ref. 7). Equation (1) has the form of a heat-diffusion equation. The left-hand side describes heat diffusion due to a gradient of T_e, the first term on the right-hand side is a source term describing Joule heating, whereas the second term accounts for the heat transfer from the electron to the phonon system due to electron–phonon scattering. The inset of Fig. 3 shows the calculated temperature profile along the wire for the three different samples.

For the long wire limit ($L\gg l_{e-ph}$), the influence of the contact pads can be neglected and the electron temperature is nearly constant over the whole wire except close to the reservoirs, where T_e drops to the lattice temperature (inset of Fig. 3, upper curve). Therefore, the left-hand side of Eq. (1)
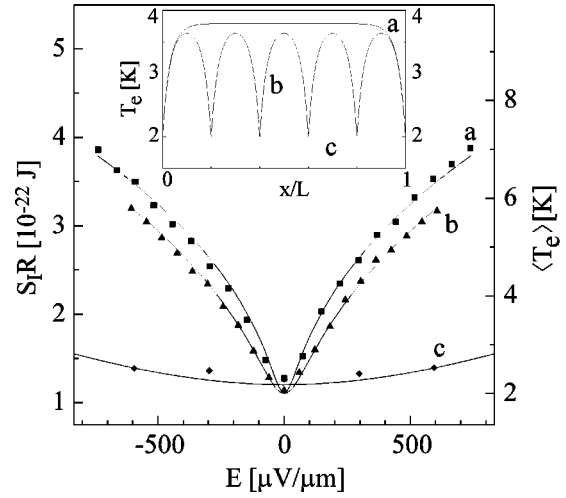
can be omitted for long wires and $S_I=4k_B(T_{ph}^5 + (e\epsilon/k_B)^2/\Gamma)^{1/5}/R$. Using this approximation curve a was calculated, which shows very good agreement with the experiment since, for large voltages $T_e\gg T_{ph}$, we obtain the dependence $T_e\propto\epsilon^{2/5}$ in this limit.[3] Even for the comparatively high phonon temperature of 2 K, a current of only 3 μA (corresponding to $\epsilon\simeq50\ \mu$V/μm) leads to an increase of T_e of $\simeq25\%$ above T_{ph}. The heating effect becomes even more pronounced at lower temperatures. For $T_{ph}=0.3$ K, Eq. (1) predicts for sample A a doubling of the mean electron temperature to 0.6 K induced by a current of only 300 nA.

If $L\simeq l_{e-ph}$, the influence of the contact pads can no longer be neglected and leads to a cooling of the electrons close to the reservoirs. In this intermediate regime, Eq. (1) has to be solved numerically, taking into account all three terms. The reservoirs in a sample with N wires of length L effectively reduce the mean electron temperature compared to a single wire of length $N\times L$, although the overall resistance is the same (inset of Fig. 3). This cooling effect is clearly seen when comparing curve b with curve a in Fig. 3. The corresponding theoretical curve was obtained by solving Eq. (1) numerically and averaging the electron temperature T_e over the whole wire. The agreement with the experimental data points is, again, very satisfactory. The fits for samples A and B yield similar values for the electron–phonon coupling parameter: $\Gamma\simeq5\times10^9$ K^{-3} m^{-2}, corresponding to $l_{e-ph}\simeq7\ \mu$m at 2 K. Our value of Γ is in agreement with the values for Cu and Ag from Refs. 3 and 6.

For sample C (30 wires with 0.84 μm length), the cooling of the reservoirs is so effective that nearly no heating takes place for the electric fields shown in Fig. 3. Nevertheless, T_e^2 varies along the wire and assumes a parabolic shape. Since $L\ll l_{e-ph}$ for each individual wire, the second term on
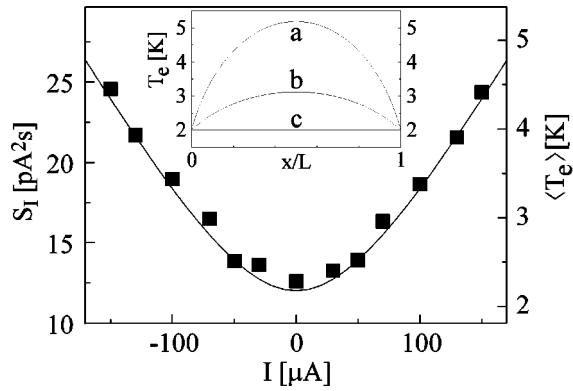
FIG. 4. Noise measurement of sample C of Fig. 3 (30 wires in series with a length of 840 nm). The solid line is the prediction of Eq. (2), which has no adjustable fit parameter. The inset shows the temperature profile of a single wire for 0, 75, and 150 μA (from bottom to top).

the right-hand side of Eq. (1) can be neglected and one obtains, after spatial averaging,

$$S_I = (2k_B T_{ph}/R)[1 + (\nu + 1/\nu)\arctan \nu], \quad (2)$$

where $\nu = \sqrt{3}eV/2\pi k_B T_{ph}$. This leads to $S_I = (\sqrt{3}/4)2eI$, i.e., $\langle T_e \rangle \propto V$, for $eV \gg k_B T_{ph}$.

The measured noise for sample C in a wider current interval is shown in Fig. 4. The size of the squares represents the measurement accuracy. As expected for $eV \gg k_B T_{ph}$, a roughly linear variation of S_I is found at higher currents. For lower currents, S_I rounds off and approaches the equilibrium thermal noise. The whole current range is accurately described by Eq. (2), which contains no adjustable fit parameters. This proves that electron–phonon scattering can be

neglected in a metallic wire of this length at 2 K. Curves a, b, and c of the inset show the calculated temperature profiles for 150, 75, and 0 μA, respectively.

In conclusion, we have demonstrated that noise measurements are a powerful tool to obtain information on electron heating effects in narrow metal wires. The measured electron temperatures are in excellent agreement with model calculations for all wire lengths ranging from $L \gg l_{e-ph}$ to $L \ll l_{e-ph}$. The experiments demonstrate that electron heating depends crucially on the length of the wires and the presence of thermal reservoirs. Hence, our results have important implications for the sample layout of electric microcircuits at low temperatures.

[1] L. W. Molenkamp and M. J. M. de Jong, Solid-State Electron. **37**, 551 (1994); M. J. M. de Jong and L. W. Molenkamp, Phys. Rev. B **51**, 13 389 (1995).

[2] A. Mittal, R. G. Wheeler, M. W. Keller, D. E. Prober, and R. N. Sacks, Surf. Sci. **361/362**, 537 (1996).

[3] M. L. Roukes, M. R. Freeman, R. S. Germain, R. C. Richardson, and M. B. Ketchen, Phys. Rev. Lett. **55**, 422 (1985).

[4] For a recent review, see M. J. M. de Jong and C. W. J. Beenakker, in *Mesoscopic Electron Transport*, edited by L. P. Kouwenhoven, G. Schön, and L. L. Sohn, NATO ASI Series E (Kluwer, Dordrecht, to be published) and the references therein.

[5] This is true if $\hbar\omega \ll kT$ or eV.

[6] A. H. Steinbach, J. M. Martinis, and M. H. Devoret, Phys. Rev. Lett. **76**, 3806 (1996).

[7] F. C. Wellstood, C. Urbina, and J. Clarke, Phys. Rev. B **49**, 5942 (1994).

[8] K. E. Nagaev, Phys. Rev. B **52**, 4740 (1995).